The EMBO Journal (2007) 26, 4487–4500 | © 2007 European Molecular Biology Organization | All Rights Reserved 0261-4189/07
www.embojournal.org

THE EMBO JOURNAL

Activation of the Cdc42p GTPase by cyclin-dependent protein kinases in budding yeast

Richelle Sopko[1], Dongqing Huang[1], Jeffrey C Smith[2], Daniel Figeys[2] and Brenda J Andrews[1,3,*]

[1]Department of Medical Genetics and Microbiology, University of Toronto, Toronto, Ontario, Canada, [2]Faculty of Medicine, Ottawa Institute of Systems Biology, University of Ottawa, Ottawa, Ontario, Canada and [3]Banting and Best Department of Medical Research, University of Toronto, Toronto, Ontario, Canada

Cyclin-dependent kinases (CDKs) trigger essential cell cycle processes including critical events in G1 phase that culminate in bud emergence, spindle pole body duplication, and DNA replication. Localized activation of the Rho-type GTPase Cdc42p is crucial for establishment of cell polarity during G1, but CDK targets that link the Cdc42p module with cell growth and cell cycle commitment have remained largely elusive. Here, we identify the GTPase-activating protein (GAP) Rga2p as an important substrate related to the cell polarity function of G1 CDKs. Overexpression of *RGA2* in the absence of functional Pho85p or Cdc28p CDK complexes is toxic, due to an inability to polarize growth. Mutation of CDK consensus sites in Rga2p that are phosphorylated both *in vivo* and *in vitro* by Pho85p and Cdc28p CDKs results in a loss of G1 phase-specific phosphorylation. A failure to phosphorylate Rga2p leads to defects in localization and impaired polarized growth, in a manner dependent on Rga2p GAP function. Taken together, our data suggest that CDK-dependent phosphorylation restrains Rga2p activity to ensure appropriate activation of Cdc42p during cell polarity establishment. Inhibition of GAPs by CDK phosphorylation may be a general mechanism to promote proper G1-phase progression.

The EMBO Journal (2007) **26,** 4487–4500. doi:10.1038/sj.emboj.7601847; Published online 13 September 2007
Subject Categories: cell & tissue architecture; cell cycle
Keywords: cell polarity; cyclin-dependent kinases; G1 phase; GTPase-activating proteins; phosphorylation

Introduction

All cells can polarize, either to adapt to changes in the extracellular environment or in response to internal cues (Pruyne and Bretscher, 2000a, b). Cell transformation and enhanced metastatic potential also demand alterations of the actin cytoskeleton, which in its normal context is dynamically rearranged during the cell cycle to ensure proper cell polarity, division, motility, and survival. For example, members of the Rho family of small GTPases, which are critical intracellular mediators of actin-modeling events, have been causally linked, either directly or through their effectors, to oncogenic transformation and metastasis (Clark *et al*, 2000; Pawlak and Helfman, 2001; Frame and Brunton, 2002).

As for other fundamental biological processes, studies using the budding yeast *Saccharomyces cerevisiae* have identified many of the conserved regulators controlling cell polarity. The budding yeast orients its growth every cell cycle toward a specific site, ultimately leading to the formation of a daughter cell. An essential and well-characterized event required for polarization of growth in eukaryotic cells is the local activation of the conserved Rho-type GTPase Cdc42p (Johnson, 1999; Etienne-Manneville, 2004). The regulated cycling of Cdc42p between GTP- and GDP-bound states is perpetuated by the antagonistic activity of two types of factors, guanine-nucleotide exchange factors (GEFs) and GTPase-activating proteins (GAPs). The sole GEF for Cdc42p, Cdc24p, functions to restrict Cdc42p activity to a single concentrated region at the plasma membrane. In haploid yeast cells, Cdc24p is kept sequestered in the nucleus via a physical interaction with Far1p (Toenjes *et al*, 1999; Nern and Arkowitz, 2000; Shimada *et al*, 2000). In G1 phase of the cell cycle, Cln–Cdc28p cyclin-dependent kinases (CDKs) phosphorylate and trigger the degradation of Far1p, allowing Cdc24p to exit the nucleus (Henchoz *et al*, 1997). In a process requiring the adaptor protein Bem1p, Cdc24p is recruited to local sites at the plasma membrane in a Cln–Cdc28p-dependent and actin-independent process, leading to the scaffold-mediated 'symmetry breaking' and local activation and cycling of Cdc42p (Butty *et al*, 2002; Irazoqui *et al*, 2003; Shimada *et al*, 2004). While only one GEF for Cdc42p has been uncovered in yeast, four GAPs—Rga1p, Rga2p, Bem3p, and Bem2p—can stimulate the hydrolysis of Cdc42-GTP *in vitro* (Marquitz *et al*, 2002; Smith *et al*, 2002). Although genetically redundant for viability, all four GAPs have different localization patterns through the cell cycle, suggesting distinct functional roles (M Peter and E Bi, personal communication). Despite their clear importance, the influence of the various GAPs on the proper localization and timing of Cdc42p activation *in vivo* remains poorly understood.

G1-specific forms of the CDKs Cdc28p and Pho85p are required for early cell cycle progression in yeast. Cdc28p and Pho85p phosphorylate multiple targets to allow proper coordination of morphogenesis, budding, DNA replication, and other events associated with commitment to the mitotic cell cycle (Moffat *et al*, 2000; Bloom and Cross, 2007). These events include, but are not restricted to, (1) the phosphorylation of the transcriptional repressor Whi5p to initiate G1 phase-specific transcription (Costanzo *et al*, 2004; de Bruin *et al*, 2004; D Huang and BJ Andrews, unpublished) and (2) the phosphorylation of Far1p, leading to release of Cdc24p

*Corresponding author. Molecular and Medical Genetics, University of Toronto, 160 College Street, CCBR, Room 1308, Toronto, Ontario, Canada M5S 3E1. Tel.: +1 416 978 8562; Fax: +1 416 946 8253; E-mail: brenda.andrews@utoronto.ca

Received: 9 March 2007; accepted: 10 August 2007; published online: 13 September 2007

©2007 European Molecular Biology Organization

from the nucleus. Targeting of Far1p, however, is unlikely the sole role for the Cln–Cdc28p CDKs in regulating unidirectional growth, since a cytoplasmic form of Cdc24p is unable to induce polarization of growth in the absence of the Cdc28p G1 cyclins (Nern and Arkowitz, 2000). The G1-specific Cdc28p cyclins (Clns) are also required for the formation of localized Cdc42p-GTP (Gulli *et al*, 2000). Indeed cells lacking a burst of late-G1 cyclin–CDK activity fail to properly orient growth and undergo morphogenetic catastrophe, halting the cell cycle at the morphogenesis checkpoint in G2 phase (Moffat and Andrews, 2004).

We used a functional genomics approach to identify new targets of G1-specific CDKs involved in polarized cell growth (Sopko *et al*, 2006). A systematic synthetic dosage lethality (SDL) screen identified the Cdc42p GAP Rga2p as a potential substrate of Pho85p (Sopko *et al*, 2006). Here, we demonstrate that G1-specific forms of both Pho85p and Cdc28p phosphorylate and inhibit Rga2p to contribute to the appropriate activation of Cdc42p. Inhibition of GAPs by CDKs may be a general mechanism linking cell polarity regulation with cell cycle progression.

Results

Orthogonal genomic data sets implicate Rga2p as a Pho85 target

We combined an automated yeast genetics platform called synthetic genetic array (SGA) analysis with a yeast overexpression array, to enable a systematic approach to examine SDL interactions. Array-based SDL screens permit systematic analysis of gain-of-function phenotypes and are based on the idea that deleterious effects of gene overexpression are often seen only in specific genetic backgrounds (Sopko *et al*, 2006). With this in mind, we screened a strain deleted for the *PHO85* CDK and discovered 65 genes that cause lethality or slow growth specifically in the absence of the kinase (Sopko *et al*, 2006). We reasoned that since many known Pho85p substrates are negatively regulated by phosphorylation, an SDL interaction might reflect an accumulation of unmodified substrate. Consistent with this idea, the SDL data set was highly enriched for known *in vivo* substrates of the Pho85p kinase. To aid prioritization of other SDL hits for follow-up studies, we compared the *pho85*Δ SDL profile to the spectrum of *in vitro* substrates for various forms of Pho85p identified using proteome chips coupled with *in vitro* kinase assays (Ptacek *et al*, 2005). Several proteins were identified in both screens, including the calcium-responsive transcription factor, Crz1p, which we confirmed as a previously unappreciated *in vivo* target of Pho85p using a variety of assays (Sopko *et al*, 2006). The GAP, Rga2p, was another protein identified in both the SDL and proteome chip screens (Ptacek *et al*, 2005; Sopko *et al*, 2006). *RGA2* is one of four genes in yeast encoding GAPs that act specifically to stimulate GTP hydrolysis by the Rho-type GTPase Cdc42p (Smith *et al*, 2002). Cdc42p-mediated GTP hydrolysis appears critical for the propagation and/or dissolution of an interaction between Cdc42p and downstream effectors, ultimately leading to the firing of specific pathways such as septin ring and actin filament assembly and organization. The results of our large-scale screens suggest that Pho85p-dependent phosphorylation of Rga2p may explain the clear role for Pho85p in cell polarity and morphogenesis, for which key substrates remain unidentified, an idea that we chose to explore.

Overexpression of RGA2 in G1 cyclin mutants produces a G1 morphology and slow-growth phenotype

We reasoned that if Pho85p were phosphorylating Rga2p *in vivo*, a specific Pho85p–cyclin complex might be involved. Since Pho85p has a clear role in regulating morphogenesis in G1 phase (Moffat and Andrews, 2004), we chose to focus on G1-specific forms of Pho85p as potential Rga2p kinases. We predicted that, like the *pho85*Δ kinase mutant, *RGA2* overexpression in a mutant lacking the relevant Pho85p cyclin(s) would result in a significant fitness defect. Pho85p is activated by three G1-specific cyclins, Pcl1p, Pcl2p, and Pcl9p, and we found that overexpression of *RGA2* produced a growth defect in strains deleted for various combinations of these G1 cyclins (Figure 1A, *pcl1*Δ, *pcl2*Δ, and *pcl9*Δdouble and triple mutants). The overexpression of *RGA2* in other Pho85p cyclin mutant backgrounds failed to have any discernable effect (data not shown). Effects in single mutants were less dramatic, consistent with the documented genetic redundancy of these G1 cyclins (Measday *et al*, 1997; Huang *et al*, 2002). We saw a similar inhibition of growth when *RGA2* was overexpressed in a strain lacking *CLN1* and *CLN2*, the G1 cyclin counterparts for the CDK, Cdc28p (Figure 1A). This growth inhibition cannot be explained by an increased stability of Rga2p in these mutants, given that we saw no substantial differences in Rga2p levels in these mutants by Western blot (Supplementary Figure 1). A significant fraction of the double and triple *cln*Δ and *pcl*Δmutants overexpressing *RGA2* arrested with a large, round unbudded cell morphology (Figure 1B, *pcl1*Δ*pcl2*Δ*:* 37%, *pcl1*Δ*pcl9*Δ*:* 33%, and *pcl1*Δ*pcl2*Δ *pcl9*Δ*:* 40%). This morphogenetic defect is similar to that seen in mutant strains bearing *cdc24* loss-of-function alleles (Hartwell *et al*, 1974; Sloat *et al*, 1981; Zheng *et al*, 1994). Since Cdc24p, the GEF for Cdc42p, opposes the function of Cdc42p GAPs, our genetic results suggest that Rga2p is hyperactive when overexpressed in G1 CDK mutants.

G1-specific Pho85p cyclins have overlapping localization with Rga2p and interact physically with Rga2p

Rga2p localizes to sites of polarized growth including the incipient bud site and bud tip, as well as the bud neck (Caviston *et al*, 2003). Coincident localization of Rga2 with relevant *in vivo* kinases should be detectable, and Pcl1p and Pcl2p are known to localize to the same regions of polarized growth (Figure 2A; Moffat and Andrews, 2004). Given the genetic redundancy we detected for *RGA2* SDL phenotypes, we asked if, like Pcl1p and Pcl2p, a GFP-tagged version of Pcl9p had overlapping localization with Rga2p (Figure 2A). We identified the bud neck and incipient bud site as the principal sites of Pcl9p localization (Figure 2A). Together with our genetic observations, these localization data suggest the G1-specific Pcls are the relevant cyclins for targeting Pho85p-dependent phosphorylation of Rga2p.

The physical interaction of kinases and their substrates can often be detected directly by copurification of the proteins or indirectly by association of kinase activity with the substrate. In particular, cyclins are known to function as substrate-targeting subunits (Miller and Cross, 2001), and several interactions between cyclins and Pho85p targets have been

 ©2007 European Molecular Biology Organization

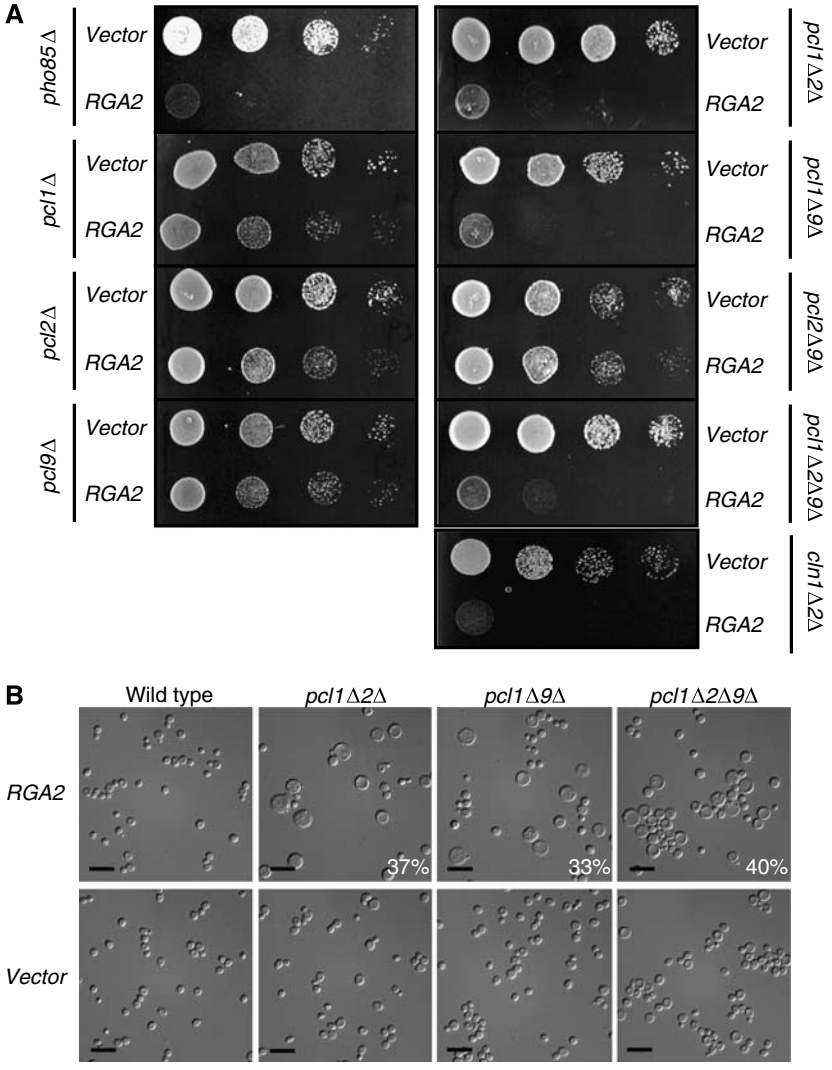

Figure 1 G1 cyclin mutants are sensitive to overexpression of *RGA2*. (**A**) Growth defect caused by overexpression of *RGA2* in the absence of *PHO85*, *PHO85* G1 cyclins, or *CDC28* G1 cyclins. Isogenic wild-type, *pho85*Δ, *pcl1*Δ, *pcl2*Δ, *pcl9*Δ, *pcl1*Δ*pcl2*Δ, *pcl2*Δ*pcl9*Δ, *pcl1*Δ*pcl9*Δ, *pcl1*Δ*pcl2*Δ*pcl9*Δ, and *cln1*Δ*cln2*Δ strains bearing either pGST-*RGA2* or vector were spotted in serial 15-fold dilutions on medium containing galactose and incubated at 30°C for 72 h. (**B**) Overexpression of *RGA2* in G1 phase-specific Pho85p cyclin mutants results in an accumulation of large, round, and unbudded cells. The morphology of those strains (top panels) from panel A was examined following 72 h of growth on galactose-containing medium. Cells were visualized at ×630 magnification. Size bar is 10 μm. The number in the bottom right corner refers to the percentage of cells displaying a large, unbudded phenotype within the population relative to the vector control (bottom panel); >200 cells were counted for each sample.

reported (Huang *et al*, 1998; Friesen *et al*, 2003). We asked whether we could detect a physical interaction between Rga2p and any of the G1-specific Pho85p cyclins. We used a FLAG-tagged version of *RGA2* to efficiently immunoprecipitate full-length Rga2p-FLAG from yeast extracts (Figure 2B, lanes 5–8). We detected copurification of Rga2p-FLAG and Pcl1p, Pcl2p, or Pcl9p from extracts prepared from strains expressing *13xMYC-PCL1*, *13xMYC-PCL2*, or 13x*MYC-PCL9* (Figure 2B, lanes 6–8, respectively). These data suggest a direct physical interaction between Rga2p- and G1-specific Pcl cyclins, consistent with a role for the Pcls in targeting Rga2p to the Pho85p kinase.

G1-specific CDK complexes phosphorylate Rga2p at distinct sites in vitro and in vivo

Rga2p possesses 18 potential CDK phosphorylation sites (S/TP; Figure 3A). Using five purified Rga2p protein fragments (Figure 3A, bottom) we performed *in vitro* kinase assays with recombinant Pho85p–Pcl and Cdc28p–Cln complexes to hone in on relevant sites of CDK phosphorylation. Fragments Rga2_2 and Rga2_4, both of which contain small clusters of S/TP sites, were excellent *in vitro* substrates for Pho85p–Pcl1p (data not shown), Pho85p–Pcl2p (Figure 3B), or Pho85p–Pcl9p (data not shown), while Cdc28p–Cln2p detectably phosphorylated all Rga2p peptides except Rga2_5 (Figure 3C). Interestingly, Rga2_5, the peptide encompassing the GAP domain failed to be efficiently phosphorylated by any of the kinases. Coomassie Blue-stained gels corresponding to these autoradiographs are included in the Supplementary data for reference (Supplementary Figure 2). We subjected the *in vitro* phosphorylated peptides to mass spectrometry analysis and identified nine sites within the Rga2_2 and Rga2_4 peptides (T320, S330, S334, T561, S692, S763, S770, S772, and T779) that were phosphorylated by

©2007 European Molecular Biology Organization

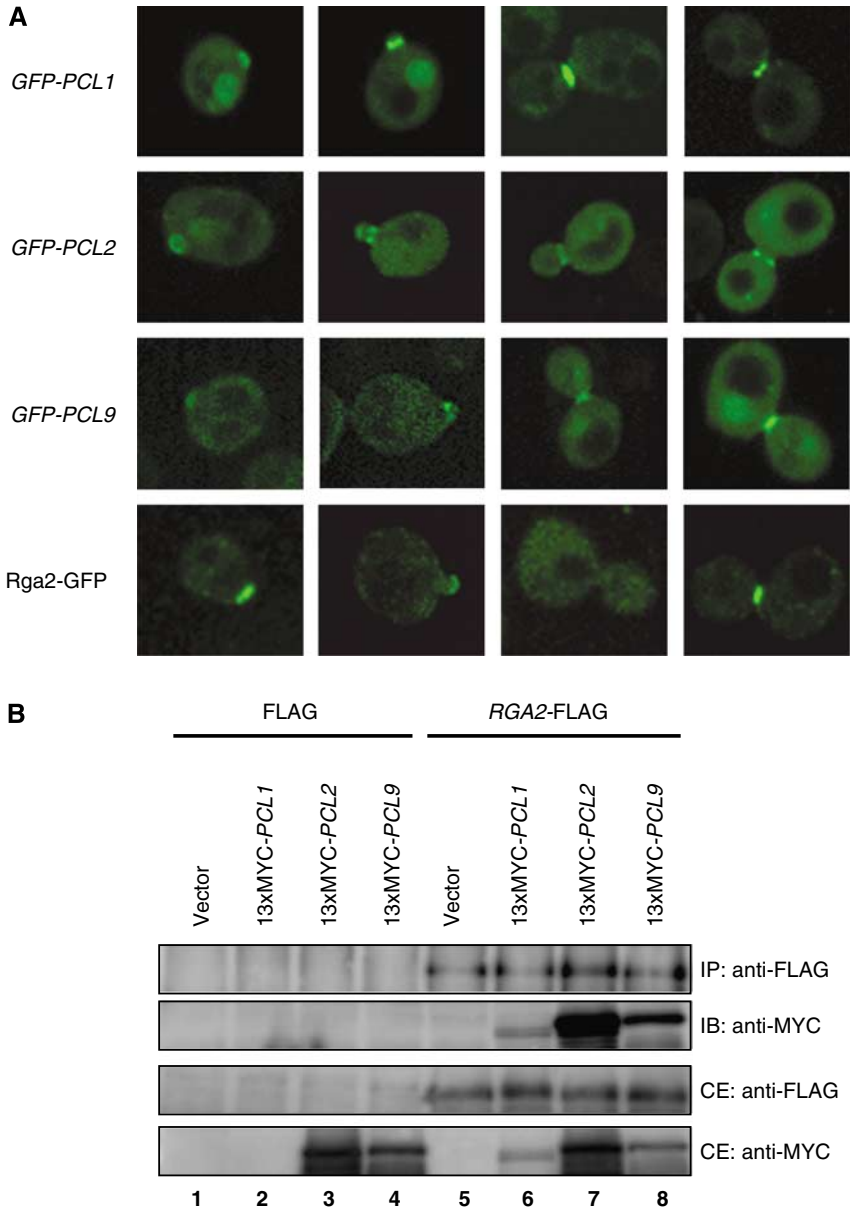

Figure 2 G1-specific Pho85 cyclins have overlapping localization and interact physically with Rga2p. (**A**) Localization of G1-specific Pho85 cyclins to sites of polarized growth. The localization of GFP-tagged Pcls was examined by confocal microscopy following expression of *GFP-PCL1*, *GFP-PCL2*, or *GFP-PCL9* from their native promoters on high-copy plasmids. The localization pattern of Rga2p-GFP expressed from its native chromosomal locus is also shown (bottom). (**B**) Co-immunoprecipitation of G1-specific Pcl cyclins with Rga2p. Extracts from strains coexpressing FLAG and vector, or *RGA2*-FLAG and vector (lanes 1 and 5, respectively); FLAG and 13xMYC-*PCL1*, or *RGA2*-FLAG and 13xMYC-*PCL1* (lanes 2 and 6, respectively); FLAG and 13xMYC-*PCL2*, or *RGA2*-FLAG and 13xMYC-*PCL2* (lanes 3 and 7, respectively); FLAG and 13xMYC-*PCL9*, or *RGA2*-FLAG and *PCL9*-13xMYC (lanes 4 and 8, respectively), were used to immunoprecipitate (IP) Rga2p. Rga2p-FLAG was detected by Western blot analysis using anti-FLAG antibodies. 13xMYC-tagged Pcls were detected by immunoblotting (IB) with anti-MYC antibodies. A total of 10% of input cell extract was loaded as a control (CE).

Pho85p–Pcl complexes *in vitro* (Table I). Five sites clustered in fragment Rga2_4 were also clearly phosphorylated *in vitro* by Cdc28p–Cln2p (S692, S763, S770, S772, and T779; Table I). Our failure to detect phosphorylated peptides by mass spectrometry on the other Rga2p fragments that were phosphorylated *in vitro* by Cdc28p (Figure 3C) may reflect variability in the kinase assay or a lack of enrichment for peptides encompassing these Rga2p fragments following protein digestion and derivatization.

Next, we sought to identify relevant *in vivo* sites of phosphorylation within Rga2p. We purified a C-terminally FLAG-tagged version of Rga2p from yeast extracts and identified eight *in vivo* sites of phosphorylation using mass spectrometry analysis (S334, S380, S692, S707, S733, S763, S770, and S772; Table I). Six of these sites were phosphorylated both *in vivo* and *in vitro* (Table I), while other phosphopeptides were detected only in one assay (*in vitro*: T320, S330, T561, and T779; *in vivo*: S380 and S707). In any case, the significant overlap between phosphorylation patterns seen in our CDK kinase assays and on Rga2p *in vivo* strongly supports the hypothesis that Rga2p is a substrate for G1 CDKs.

 ©2007 European Molecular Biology Organization

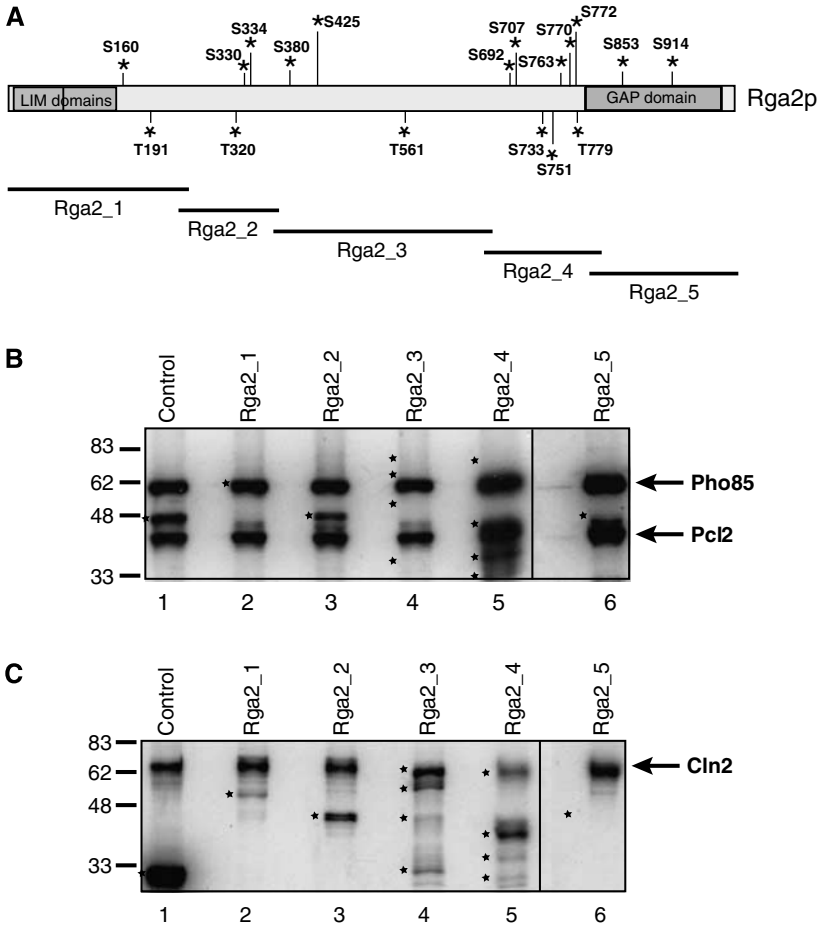

Figure 3 G1-specific CDKs can phosphorylate Rga2 *in vitro*. (**A**) Schematic representation of full-length Rga2p. Locations of potential CDK phosphorylation sites (S/TP) are indicated by asterisks. The regions of Rga2p contained in five fragments used in kinase assays are shown (Rga2_1 through Rga2_5). (**B**) Phosphorylation of Rga2p by Pcl2p-Pho85p kinase *in vitro*. The five GST-Rga2p fragments (see A) were mixed with Pcl2p–Pho85p (lanes 2–6) in kinase reactions along with [γ-^{32}P]ATP. Pho4p (lane 1) was included as a control. Phosphorylation of proteins was analyzed by SDS–PAGE and autoradiography. The position of migration of input proteins (see Supplementary Figure 2 for Coomassie Blue-stained gel) is indicated by stars. The positions of migration of phosphorylated Pcl2p and auto-phosphorylated Pho85p are indicated. (**C**) Phosphorylation of Rga2p by Cln2p–Cdc28p kinase *in vitro*. GST-Rga2p fragments were mixed with Cln2p–Cdc28p kinase (lanes 2–6) in kinase reactions. Histone H1 (lane 1) was included as a control. The position of migration of input proteins (see Supplementary Figure 2 for Coomassie Blue-stained gel) is indicated by stars. The position of phosphorylated Cln2p is indicated.

Table I Phosphorylated residues within Rga2p as identified by mass spectrometry

S/TP site	*In vitro*		*In vivo*			Mutated in Rga2^{8A}
	Cdc28–Cln2	Pho85–Pcl2	Wild type	*Pho85*Δ	*cln1*Δ*cln2*Δ	
S160						√
T191						
T320		√				
S330		√				√
S334	√	√	√		√	√
S380			√			
S425						
T561		√				
S692	√	√	√	√	√	
S707			√		√	√
S733	√		√	√	√	
S751						√
S763	√	√	√	√	√	√
S770	√	√	√	√	√	√
S772	√	√	√	√	√	√
T779	√	√				
S853						
S914						

©2007 European Molecular Biology Organization

To further test this hypothesis, we purified Rga2p protein from *pho85*Δ and *cln1*Δ*cln2*Δ mutants to assess alterations in Rga2p phosphorylation. We failed to detect phosphorylation at three sites (S334, S380, and S707; Table I) when Rga2p was purified from a *pho85*Δ strain, whereas phosphorylation of only S380 appeared dependent on *CLN1* and *CLN2* (Table I). Although we cannot exclude the possibility that an insufficient enrichment for derivatized peptides encompassing sites S380 and S707 is underrepresenting phosphorylation, we predict that a lack of phosphorylation detected at these sites is indicative of their CDK-dependent phosphorylation. On the other hand, we recovered significant derivatization of non-phosphorylated peptides encompassing S334 in *pho85*Δ, indicating that phosphorylation at this site is indeed dependent on Pho85p activity *in vivo*. The differential phosphorylation of Rga2p by Pho85p–Pcl and Cdc28p–Cln complexes suggests that these kinases may each contribute to the regulation of Rga2p via phosphorylation, both at unique and potentially overlapping sites (Table II).

Overexpression of RGA2 mutated at phosphorylation sites causes growth defects and an accumulation of large, unbudded cells

To further substantiate the view that G1 CDKs phosphorylate Rga2p to regulate its activity, we analyzed the phenotype associated with overexpression of versions of Rga2p mutated at various S/TP sites. Rather than focusing solely on those residues implicated as *in vivo* sites by our biochemical analysis, we chose a broader approach that considered potential phosphorylation sites of Rga2p conserved among fungal species, as well as sites conserved among all Cdc42 GAPs (see Figure 4A). We expressed mutant alleles of Rga2p lacking one or more of 13 different S/TP sites (S/T-A substitutions) in wild-type cells. Although S380 was phosphorylated in our wild-type Rga2p purification, we were unable to test the function of an S380A mutant as the mutant protein is unstable. Nonetheless, we predicted that expression of a hypo-phosphorylated version of *RGA2* might mimic the effect we saw when overexpressing wild-type *RGA2* in a *pho85*Δ strain or various CDK mutants. Overexpression of Rga2p mutants lacking any single site, or several double-site combinations, had no obvious phenotypic consequence relative to wild-type Rga2p (Figure 4A). Certain alanine substitution combinations, however, showed a pronounced phenotypic consequence and these effects were additive. An Rga2p mutant carrying eight substitutions (S160A, S330A, S334A, S707A, S751, S763, S770A, and S772A; hereafter referred to as Rga2^{8A}p) had the most dramatic effect on growth when overexpressed in wild-type cells (Figure 4A, *RGA2*^{8A} was expressed at levels comparable to wild-type *RGA2*; Figure 4F). The residues altered in the Rga2^{8A}p mutant include five serine residues that were phosphorylated both *in vivo* and *in vitro* (see above and Table I). Expressing *RGA2*^{8A} in wild-type cells phenocopied the overexpression of wild-type *RGA2* in CDK mutants; a large proportion (∼47%) of cells displayed a large, round unbudded cell morphology after 6 h in galactose (Figure 4B). The morphological effects of expressing quadruple- and quintuple-site mutants were similar to that of the 8 × mutant Rga2^{8A}, however more subtle. Notably, overexpression of *RGA2*^{8A} is still lethal in *pho85*Δ and *cln1*Δ*cln2*Δ mutant strains, as we would predict if these kinases were responsible for phosphorylating Rga2p (data not shown) and overexpression of *PCL1*, *PCL2*, or *PCL9* is unable to suppress *RGA2*^{8A}-associated toxicity (Supplementary Figure 3). In addition, *RGA2*^{8A} exacerbated the temperature sensitivity and unbudded phenotype of a *cdc24-4* strain (Figure 4C). Together, our biochemical and genetic data suggest that a deficiency of CDK-dependent phosphorylation of Rga2p leads to significant G1 defects, most consistent with a failure to negatively regulate Rga2p function.

Abolishment of Rga2p GAP function suppresses G1 defects of wild-type cells overexpressing RGA2^{8A}

To ask whether the phenotype displayed by wild-type cells overexpressing *RGA2*^{8A} was due to unrestricted Rga2p GAP activity, we chose to mutate a conserved lysine residue (K872) within the GAP domain of Rga2p, previously shown to be essential for activation of the mammalian RhoA GTPase by the GAP p190 (Li *et al*, 1997). Furthermore, mutation of this residue to alanine resulted in elimination of GAP activity for Rga1p, another *S. cerevisiae* Cdc42p GAP, *in vitro* (Gladfelter *et al*, 2002), and diminished the interaction between the Rga1p GAP domain and Cdc42p. Substitution of lysine 872 with alanine in Rga2^{8A}p resulted in the suppression of both the large, unbudded morphology (Figure 4B) and growth inhibition (Figure 4D) produced by *RGA2*^{8A} overexpression. Mutation of the GAP domain reduced the large cell size of *RGA2*^{8A}-expressing cells from 67 to 42 fl, near the size of cells expressing vector or wild-type *RGA2* (Figure 4E). Suppression of *RGA2*^{8A} overexpression defects by mutation of

Figure 4 Functional analysis of *RGA2* mutations. (**A**) A wild-type strain bearing either vector, p*GAL-RGA2*, or plasmids expressing *RGA2* mutated at potential CDK phosphorylation sites was spotted in serial 15-fold dilutions on galactose medium and incubated at 30°C for 72 h. The schematic of full-length Rga2p shows those potential CDK phosphorylation sites (asterisks; S/TP) mutated to alanine. The version comprising the eight alanine substitutions, S330A, S334A, S707A, S751A, S160A, S763A, S770A, S772A, is referred to as *RGA2*^{8A}. (**B**) Wild type strains carrying either vector, p*GAL-RGA2*-FLAG, p*GAL-RGA2*^{8A}-FLAG, or p*GAL-RGA2*^{8A,K872A}-FLAG were induced in galactose for 6 h and examined by microscopy. Cells were visualized at × 400 magnification. Size bar is 10 μm. The number in the bottom right corner refers to the percentage of cells displaying a large, unbudded phenotype relative to the vector control; >400 cells were counted. (**C**) A *cdc24-4* strain bearing the *RGA2*^{8A} allele at the endogenous *RGA2* locus was spotted in serial 15-fold dilutions on rich medium, and incubated at semi-permissive temperatures. Cell morphology was examined using differential interference contrast (DIC) microscopy at × 400 magnification. Size bar is 10 μm. (**D**) Wild-type strains bearing either vector, p*GAL-RGA2*, p*GAL-RGA2*^{8A}, or p*GAL-RGA2*^{8A,K872A} were spotted in serial 15-fold dilutions on galactose- (left) or glucose (right)-containing medium and incubated at 30°C for 72 h. (**E**) Wild-type cells bearing either vector, p*GAL-RGA2*, p*GAL-RGA2*^{8A}, or p*GAL-RGA2*^{8A,K872A} were grown to log phase and induced with galactose for 6 h. The cell volume distribution (fl) in culture was measured using a Coulter Z2 Particle analyzer. The median volume of cells was as follows: vector = 36 ± 5 fl; *RGA2* = 40 ± 1 fl; *RGA2*^{8A} = 67 ± 1 fl; and *RGA2*^{8A,K872A} = 42 ± 1 fl. (**F**) *RGA2*-FLAG, *RGA2*^{8A}-FLAG, and *RGA2*^{8A,K872A}-FLAG were expressed in low copy under the regulation of the *GAL1* promoter in wild-type cells. Cells were induced with galactose for 3 h. Expression was monitored by Western blot analysis with α-FLAG antibodies (top panel) and compared to levels of Swi6 detected in extracts using α-Swi6 antibodies (bottom panel).

 ©2007 European Molecular Biology Organization

the GAP domain implies that hypo-phosphorylation of Rga2p leads to hyperactive GAP function.

Levels of activated Cdc42p are reduced in CDK mutants and in wild-type cells expressing RGA2^{8A}

Rga2p normally functions to counteract Cdc42p activation. We reasoned if CDK-mediated phosphorylation of Rga2p acts to restrain its activity, then phosphorylation-deficient Rga2p should be biochemically hyperactive. To test this idea, we assessed activated Cdc42p (Cdc42p-GTP) levels in CDK mutants and cells expressing *RGA2^{8A}*. We predicted that the significant growth defects seen in *pho85*Δ or *pcl*Δ cells overexpressing *RGA2* or in wild-type cells expressing a hypo-phosphorylated derivative of Rga2p (*RGA2^{8A}*) reflect

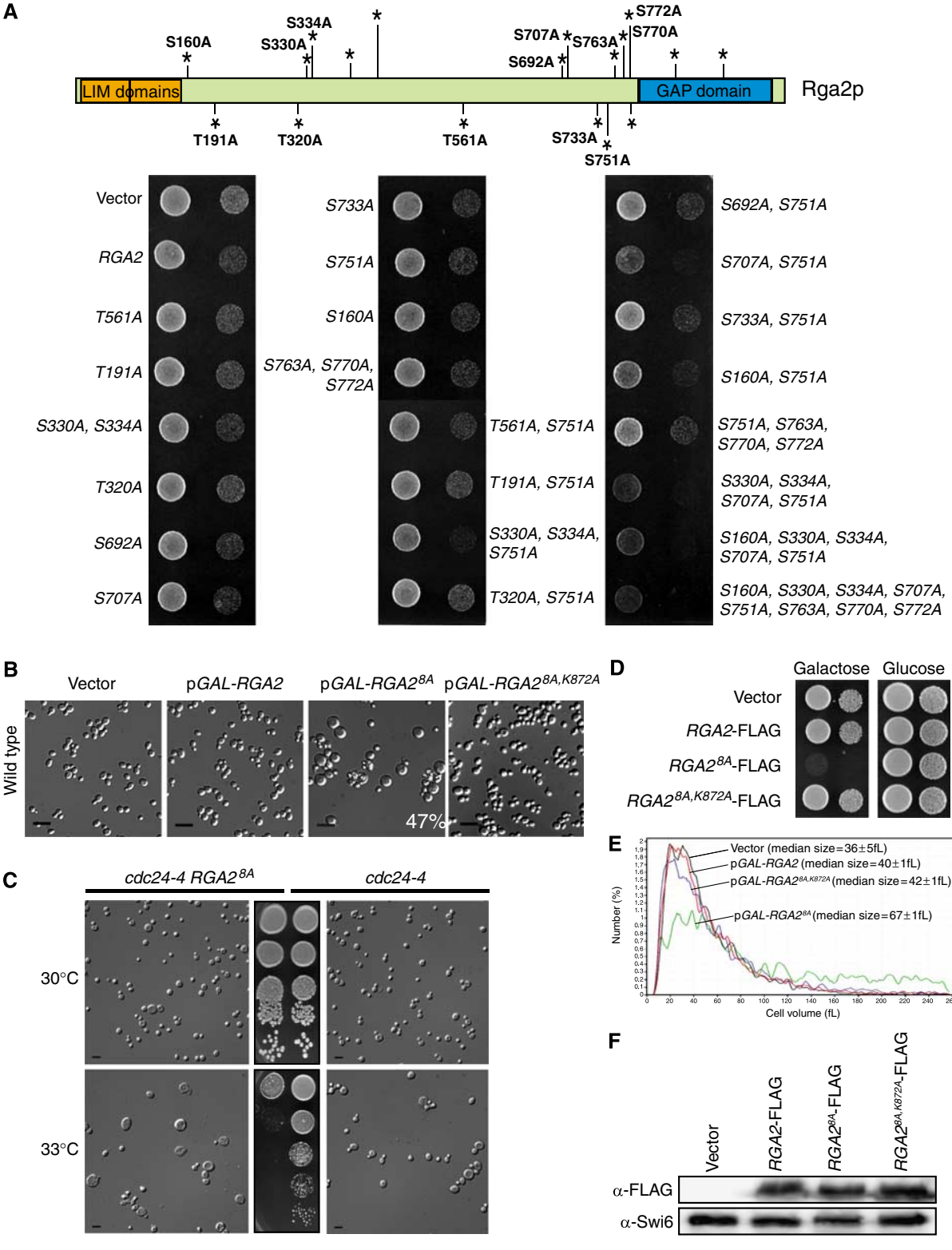

©2007 European Molecular Biology Organization

hyperactive GAP (Rga2p) activity, and would be evident as decreased levels of GTP-bound Cdc42p *in vivo*. We used a CRIB domain from the human PAK1 kinase, a known Cdc42p effector, in a GST pull-down assay to specifically recover Cdc42p-GTP from yeast cell extracts (Caviston *et al*, 2002; Aguilar *et al*, 2006). We reproducibly recover less Cdc42-GTP from CDK mutant extracts (Figure 5A, lanes 5–7), in particular from a *pho85*Δ extract (Figure 5A, lane 5; see also Supplementary Figure 4). Expression of *RGA2*^{8A} from the *RGA2* chromosomal locus has little effect on growth, unless sensitized by reduction of function of *CDC24* (Figure 4C). Consistent with this observation, we see only a slight decrease in the levels of Cdc42p-GTP when *RGA2*^{8A} is expressed at endogenous levels, compared with wild type (Figure 5A, lane 1 versus lane 2). As well, we see relatively reduced levels of Cdc42-GTP when Rga2^{8A} is the only endogenous GAP (*RGA2*^{8A}*bem3*Δ*rga1*Δ versus *rga2*Δ*bem3*Δ*rga1*Δ; Figure 5A, lane 3 versus lane 4). A shift in the amount of Cdc42p-GTP relative to total Cdc42p suggests either (1) a decrease in the activity of the Cdc42p GEF, Cdc24p, or (2) an increase in the activity of a Cdc42p GAP(s). Nonetheless, these data are consistent with our model that phosphorylation restricts Rga2p activity and that Rga2p is hyperactive in the absence of Pho85p function due to a lack of phosphorylation. This hypothesis is further strengthened by the fact deletion of *PCL1* and *PCL2* exacerbates the phenotype of a *cdc24-4* strain (Figure 5B).

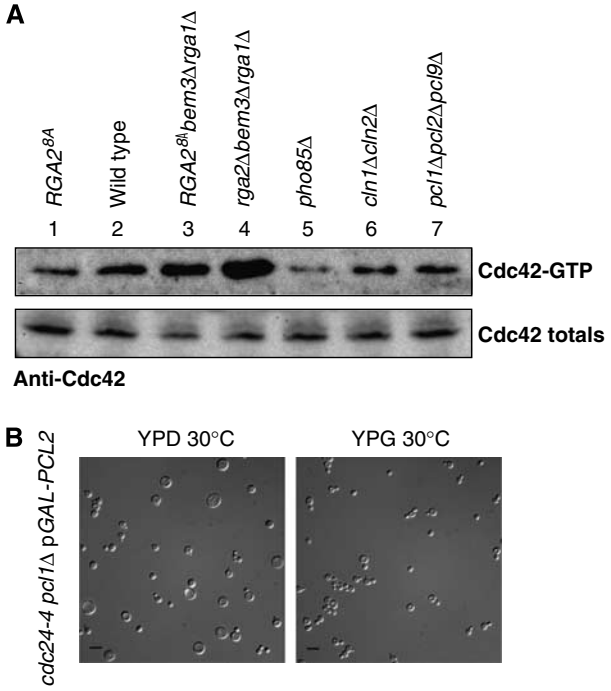

Figure 5 Levels of activated Cdc42p are reduced in CDK mutants and in wild-type cells expressing *RGA2*^{8A}. (**A**) Cell extract from a strain bearing *RGA2*^{8A} at the *RGA2* endogenous locus (lane 1), a wild-type strain (lane 2), an *RGA2*^{8A}*bem3*Δ*rga1*Δ strain (lane 3), an *rga2*Δ*bem3*Δ*rga1*Δ triple GAP mutant (lane 4), a *pho85*Δ mutant (lane 5), a *cln*Δ*cln2*Δmutant (lane 6), and a *pcl1*Δ*2*Δ*9*Δmutant (lane7) were incubated with GST-PAK (CRIB) beads that bind Cdc42-GTP. Cdc42p was detected by Western blot using α-Cdc42 antibodies. (**B**) Removal of the Pho85 G1 cyclins, *PCL1* and *PCL2*, exacerbates the phenotype of *cdc24-4* allele-bearing cells. A *cdc24-4 pcl1*Δp*GAL*-3xHA-*PCL2* strain was grown in the presence of glucose (YPD) or galactose (YPG), at a semi-permissive temperature of 30°C, and examined by microscopy. Cells were visualized at × 400 magnification. Size bar is 10 μm.

Rga2^{8A}*p fails to accumulate G1 phase-specific phosphoforms*

To substantiate the kinase–substrate relationship between G1 CDKs and Rga2p *in vivo*, we used a TAP-tagged version of Rga2p to examine Rga2p phosphoforms throughout the cell cycle. For these experiments, synchronized cells were released from a G1 arrest and samples were taken periodically for Western blotting. We found that Rga2p underwent an electrophoretic mobility shift 30–45 min after release from G1 arrest, coincident with DNA replication and bud emergence (Figure 6A). Treatment of extracts with phosphatase caused collapse of the Rga2p band, indicating that the reduced electrophoretic mobility is due to phosphorylation (Figure 6B). We assayed Rga2p phosphorylation in strains expressing an analogue-sensitive allele of *CDC28* (*cdc28*-as) or *PHO85* (*pho85*-as) that can be specifically inhibited *in vivo* with the ATP analogue 1NM-PP1 or 1Na-PP1, respectively (Bishop *et al*, 2000; Carroll *et al*, 2001). We failed to detect a substantial change in the timing or level of Rga2p phosphorylation throughout the cell cycle when either *PHO85* or *CDC28* was singly genetically impaired, either using the *as* alleles or by removing specific cyclins (Figure 6C).

We reasoned that our failure to detect an obvious change in phosphorylation in single CDK mutants reflects the clear genetic redundancy of CDK function (Moffat and Andrews, 2004). Since cells lacking all G1-CDK activity are inviable, we chose to assay cell cycle-dependent phosphorylation of Rga2^{8A}p, the version of Rga2p lacking confirmed CDK phosphorylation sites (Figure 6D). Cells expressing Rga2^{8A}p failed to accumulate G1-specific phosphoforms, suggesting that the mutant protein indeed lacks sites that are targeted for phosphorylation *in vivo*. No additional discernable shift in Rga2^{8A}p mobility was detectable when the mutant protein was expressed in *cln1*Δ*cln2*Δ cells (data not shown). These data support our hypothesis that both Pho85p and Cdc28p contribute to the phosphorylation of Rga2p in G1 phase.

The localization of Rga2p is dependent on phosphorylation by Pho85p and Cdc28p CDK complexes

As noted earlier, the localization of Rga2p is cell cycle-dependent; Rga2p localizes to the incipient bud site in unbudded cells, whereas small-budded cells display Rga2p at the bud tip. Rga2p fails to localize to any discrete region in medium-budded cells (Caviston *et al*, 2003), and relocalizes to the bud neck during mitosis (see Figure 2A). To assess whether phosphorylation plays a role in proper localization of Rga2p, we examined localization of Rga2p-GFP in various CDK and cyclin mutants. We were unable to detect any significant differences in Rga2p-GFP localization in a *pcl1*Δ*2*Δ*9*Δ, *pho85*Δ, *cln1*Δ*cln2*Δ, or a*Δpho85as* strain incubated with 25 μM analogue (data not shown). A GFP-tagged version of Rga2^{8A}p did not exhibit any observable differences in localization relative to wild-type Rga2p-GFP. Examination of Rga2^{8A}p in a *cln1*Δ*cln2*Δbackground however revealed a significantly altered localization: (1) more cells displayed signal, including medium-budded cells that do not normally have any localized Rga2p-GFP signal and (2) small and medium-budded cells had more signal along the circumfer-

 ©2007 European Molecular Biology Organization

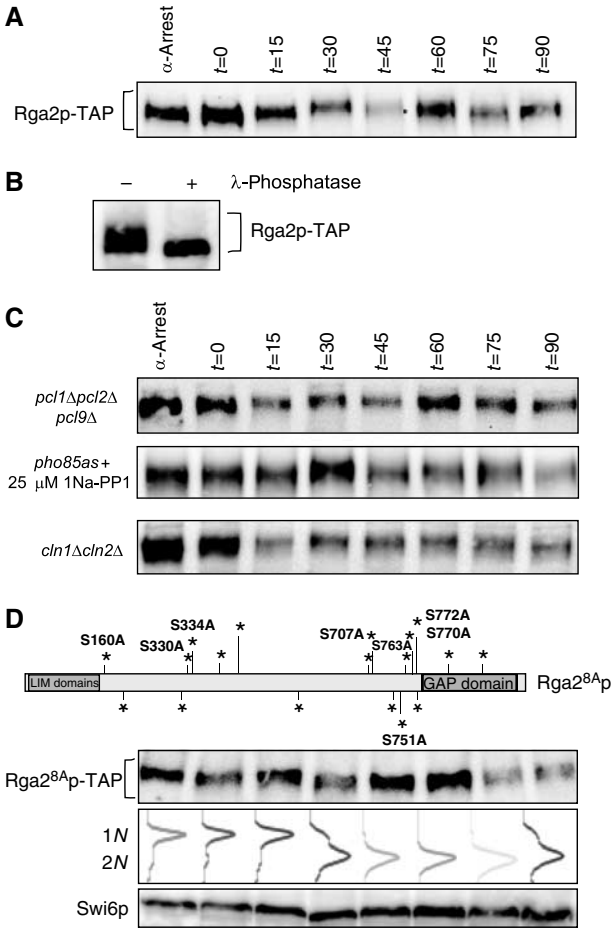

Figure 6 Rga2^{8A}p fails to accumulate G1 phase-specific phosphoforms. (**A**) The phosphorylation of Rga2p-TAP during a cell cycle was monitored by Western blotting using α-TAP antibody. Samples were taken every 15 min for 90 min following alpha-factor block and release. (**B**) Rga2p-TAP was immunoprecipitated, divided into two aliquots, and one aliquot was treated with 100 U of lambda phosphatase. (**C**) The phosphorylation of Rga2p-TAP in *pcl1*Δ*pcl2*Δ*pcl9*Δ, *pho85*-as, and *cln1*Δ*cln2*Δ cells was monitored during a cell cycle by Western blotting using polyclonal α-TAP antibodies. Samples were taken every 15 min for 90 min following alpha-factor block and release. For the *pho85*-as (analogue sensitive) strain, cells were released from alpha-factor into the indicated concentration of 1Na-PP1. (**D**) The phosphorylation of Rga2p-TAP or Rga2^{8A}p-TAP in wild-type cells was monitored during a cell cycle by Western blotting using α-TAP antibody. Samples were taken every 15 min for 90 min following alpha-factor block and release. Corresponding FACS profiles indicate relative position in the cell cycle. Western blot analysis of Swi6p was used to assess loading. The schematic of Rga2^{8A}p shows those potential CDK phosphorylation sites (asterisks; S/TP) mutated to alanine.

ence of the bud (Figure 7A). Since Rga2^{8A}p lacks abundant phosphorylation in late G1 phase, we conclude that phosphorylation of Rga2p plays a role in proper localization of this GAP.

Given that substitution of lysine 872 with alanine abrogated the effects of Rga2^{8A}p overproduction (Figure 4B, D and E) and substitution of this conserved residue has been shown to abolish GAP–Cdc42p interactions (Gladfelter *et al*, 2002), we next examined localization of Cdc42p and Rga2^{8A}p. Rga2^{8A}-GFP and mcherry-Cdc42p indeed have a largely overlapping and coincident localization along the circumference of small-budded *cln1*Δ*cln2*Δ cells (Figure 7B). This observation supports our prediction that Rga2^{8A} more readily interacts with Cdc42p. In fact, cells overexpressing *RGA2*^{8A} fail to localize Cdc42p to a discrete site as required for initiation of bud emergence (Supplementary Figure 5).

Discussion

The specific morphological events that require G1 CDK activity remain obscure. We have accumulated a substantial body of evidence that identifies the Cdc42 GAP, Rga2p, as a relevant *in vivo* target of G1 CDKs related to their established role in regulating cell polarity including: (1) *RGA2* overexpression in CDK mutant backgrounds produces a significant growth defect and depolarized growth suggestive of GAP hyperactivity; (2) Rga2p is phosphorylated by both G1-specific forms of Pho85p and Cdc28p CDKs *in vitro*, and physically associates with Pho85p cyclins; (3) Rga2p and G1 Pho85p cyclin localization overlaps at the sites of polarized growth; (4) mutation of CDK consensus sites that are phosphorylated both *in vivo* and *in vitro* results in loss of G1 phase-specific phosphorylation of Rga2p, a decrease in activated Cdc42p, and an exacerbation of *cdc24* phenotypes reflective of Rga2^{8A}p hyperactivity; and (5) a failure to completely phosphorylate Rga2p results in localization defects. Rga2p therefore provides a significant link between G1 CDK activity and the Cdc42p GTPase polarity module. Our data suggest that phosphorylation of Rga2p inhibits GAP function to contribute to appropriate activation of Cdc42p during cell polarity establishment.

Previous studies have connected G1 CDKs to activation of the Cdc42 GTPase module. For example, *pho85*, *cln1 cln2*, and *pcl1 pcl2* mutant strains show synthetic lethal interactions with specific regulators and effectors of Cdc42p (Benton *et al*, 1993; Cvrckova and Nasmyth, 1993; Lenburg and O'Shea, 2001; Moffat and Andrews, 2004). Biochemical links have also been uncovered: Rga2p can be phosphorylated by Cdc28as1p-Clb2p in whole-cell extracts (Ubersax *et al*, 2003) and other Cdc42 GAPs, Bem3p, and Rga1p, physically interact with Cdc28p–Cln2p (Archambault *et al*, 2004). While most previous work has linked only Cdc28p with Cdc42p and its regulators, our observations implicate Rga2p as a G1-specific substrate of both Cdc28p and Pho85p. Pho85p and Cdc28p, in complex with their G1 cyclins, can phosphorylate Rga2p *in vitro*, at overlapping and unique sites and some of these sites are phosphorylated *in vivo* in a CDK-dependent manner. Overexpression of *RGA2* in strains deficient in G1-specific forms of either CDK results in arrest as large, unbudded cells, similar to the effects of *CDC24* GEF inactivation. Also, we were unable to abolish accumulation of Rga2p G1-phase phosphoforms by impairing either kinase alone. Together, these results suggest that additive phosphorylation by Cdc28p and Pho85p contributes to inhibition of Rga2p activity, perhaps by regulating distinct aspects of Rga2p function. A partnership between CDKs in regulating cell cycle and cell polarity targets is an emerging theme in G1 regulation. Both Cdc28p and Pho85p are involved in phosphorylation of the S-phase CDK inhibitor Sic1, which primes the protein for degradation (Schwob *et al*, 1994; Nishizawa *et al*, 1998). Likewise, both CDKs are required for relieving inhibition of G1 transcription factors by the Whi5p repressor, by impacting different facets of Whi5p function (Costanzo

©2007 European Molecular Biology Organization

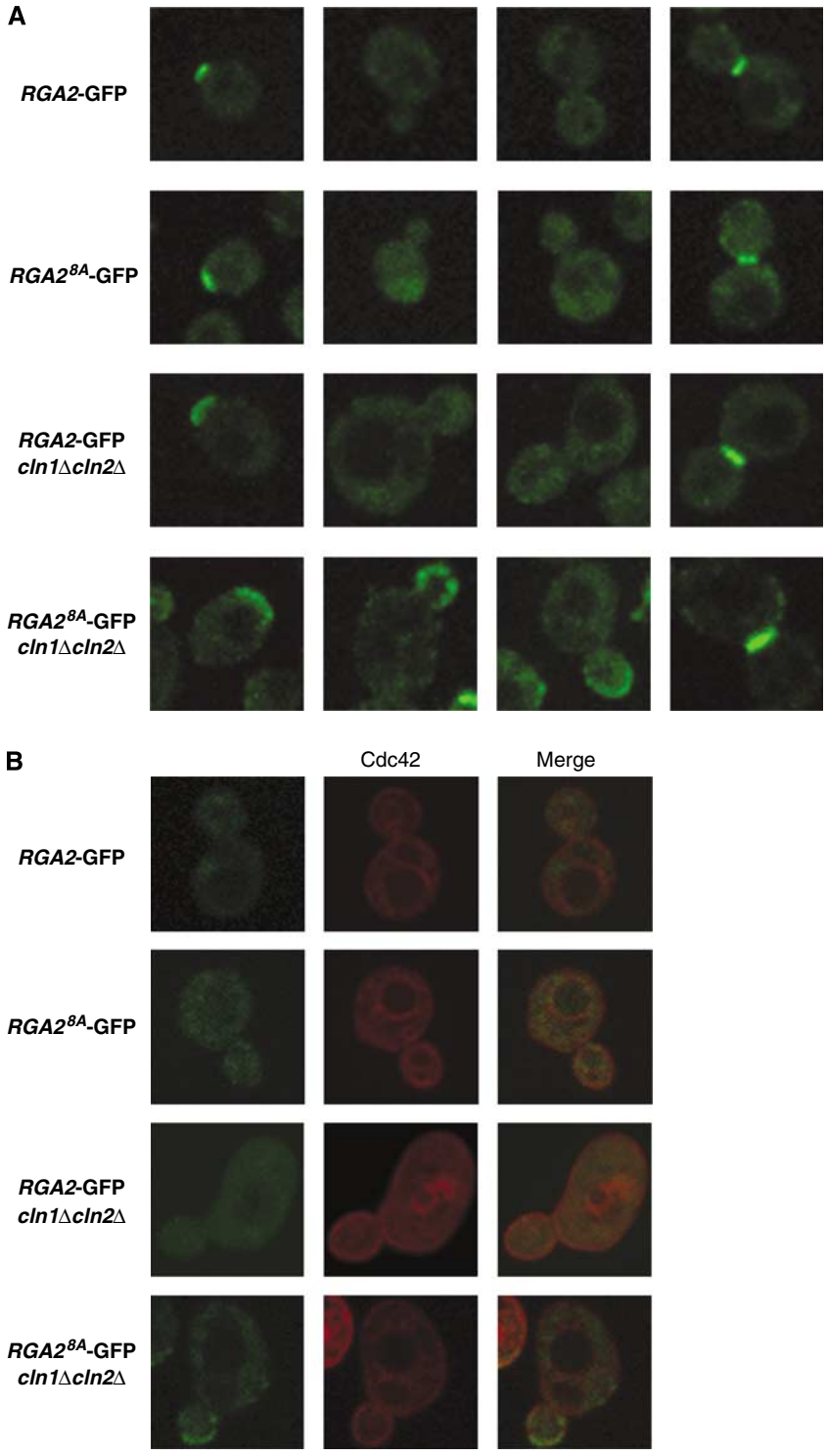

Figure 7 Localization of Rga2p in late G1 phase is dependent on phosphorylation by Pho85p and Cdc28p CDK complexes. (**A**) Phosphorylation influences the localization of Rga2p in *cln1*Δ*cln2*Δ cells. Wild-type cells expressing *RGA2*-GFP or *RGA2*^{8A}-GFP, and *cln1*Δ*cln2*Δ cells expressing *RGA2*-GFP or *RGA2*^{8A}-GFP were examined using spinning-disc confocal microscopy. Individual cells representing various stages of the cell cycle are highlighted. (**B**) *RGA2*^{8A} shares overlapping localization with Cdc42p in *cln1*Δ*cln2*Δ cells. Those strains from panel A were transformed with p*MET*-mcherry-*CDC42* and examined using spinning-disc confocal microscopy.

et al, 2004; de Bruin *et al*, 2004; D Huang and BJ Andrews, unpublished). Dual regulation by CDKs or other partner kinases may prove to be a common feature of cell cycle regulatory transitions that must be both rapid and responsive. Also, multi-site phosphorylation by one or more kinases may prove to be the rule, rather than the exception, among CDK targets including Rga2p. In fact, a recent computational analysis showed enrichment of multiple closely spaced consensus sites for Cdc28p substrates in yeast, a pattern that proved predictive of likely CDK targets (Moses *et al*, 2007).

 ©2007 European Molecular Biology Organization

The apparent redundancy of Rga2p regulation is also evident through mutational analysis of phosphorylation sites. We analyzed the effects of mutating potential phospho-sites in Rga2p to alanine, in an effort to mimic a non-phosphorylatable residue. We reasoned that if phosphorylation at any particular site was important for Rga2p regulation, overexpression of the relevant phospho-site mutant in otherwise wild-type cells should phenocopy the SDL and morphology defect triggered by overproduction of Rga2p in the associated kinase mutant. We focused our mutagenesis on 13 of the 18 potential phosphorylation sites (S/TP) of Rga2p that are conserved either amongst three *Saccharomyces sensu stricto* species (*Saccharomyces mikatae*, *Saccharomyces paradoxus*, and *Saccharomyces bayanus*) or among other Cdc42p GAPs. Most of the sites fall within two 'clusters', one near the LIM domain at the N-terminus of Rga2p, and the other adjacent to the GAP domain at the C-terminus (see Figure 3A). Despite the clear conservation, mutation of any single phosphorylation site in Rga2p was of little phenotypic consequence. Rather, we saw a cumulative effect on growth and cell polarity as additional sites were mutated—overproduction of Rga2^{8A}p, which carries eight substitutions in both clusters, caused a cell polarity and growth defect comparable to that seen when wild-type *RGA2* is overexpressed in CDK mutants.

What are the functional consequences of Rga2p phosphorylation? Our genetic and biochemical data suggest that a failure to phosphorylate Rga2p results in Rga2p GAP hyperactivity and a consequent inability to appropriately activate Cdc42p. First, elimination of GAP activity by mutation of the Rga2p GAP domain restored wild-type growth and morphology to *RGA2^{8A}*-expressing cells. Second, Cdc42p-GTP levels were dramatically reduced in extracts from a *pho85*Δ mutant, implicating G1 Pho85p CDK complexes specifically. Third, expression of a hypo-phosphorylated version of Rga2p (Rga2^{8A}p) also decreased levels of activated Cdc42p and exacerbated *cdc24* mutant defects, consistent with GAP hyperactivity. We note that cells exhibit considerable tolerance for reduced levels of Cdc42p-GTP, emphasizing the robust nature of the Cdc42p regulatory pathway. A failure to properly inhibit Rga2p may explain previous genetic links between Pho85p and Cdc42p. Deletion of *PHO85* causes lethality in a *cdc42-1* strain, which has reduced levels of Cdc42p, and arrests with a large, unbudded cell morphology at the restrictive temperature (Kozminski *et al*, 2000; Huang *et al*, 2002). The *cdc42-1* strain may be poised on the brink, and a further reduction in Cdc42p-GTP levels due to hyperactive Rga2p in the *pho85* deletion strain may be catastrophic.

In addition to the possibility that phosphorylation affects Rga2p GAP activity directly, we entertained the idea that phosphorylation may contribute to the localization of Rga2p. Phosphorylation of the Rho1p-GEF, Tus1p, by Cdc5p is required for localization to the bud neck at cytokinesis (Yoshida *et al*, 2006). We however saw no apparent change in Rga2p localization when Cdc28p or Pho85p was separately impaired. Rather, the combination of a hypo-phosphorylated version of Rga2p (Rga2^{8A}p) with deletion of *CLN1* and *CLN2* produced obvious localization defects. Despite this abnormal localization, and a clear deficiency in G1-specific phosphorylation of Rga2p (Figure 6D), *RGA2^{8A}cln1*Δ*cln2*Δ cells initiate bud formation normally, suggesting that G1 CDKs contribute to the formation of Cdc42p-GTP through other mechanisms besides downregulation of Rga2p. Consistent with this, a strain in which Rga2^{8A}p is the only GAP available for Cdc42p (an *RGA2^{8A}rga1*Δ*bem3*Δ triple mutant) can still polarize growth (data not shown), albeit erratically as seen for *rga2*Δ*rga1*Δ*bem3*Δ mutants (Smith *et al*, 2002). Likely CDK targets include other factors that contribute to the generation of Cdc42-GTP, such as the other Cdc42p GAPs Bem2p and Bem3p (M Knaus and M Peter, personal communication), which would explain why CDK mutants display a more dramatic reduction in the levels of Cdc42-GTP than that caused by *RGA2^{8A}* expression (Figure 5A). In addition, G1 CDKs have been shown to phosphorylate the polarity proteins Boi1p and Boi2p (McCusker *et al*, 2007), and the septin Shs1p (D Kellogg, personal communication), which likely contribute to efficient polarization. Genetic data suggest that more CDK targets remain to be discovered.

The persistence of Rga2^{8A}p at the cortex of budded *cln1*Δ*cln2*Δcells suggests that hypo-phosphorylated Rga2p can still interact physically with Cdc42p. Rga2^{8A}p may remain inappropriately associated with Cdc42p, since Cdc42p laterally diffuses throughout the plasma membrane of enlarging buds (Richman *et al*, 2002). A prolonged interaction of Rga2^{8A}p and Cdc42p may prevent Cdc42p activation, resulting in a failure to polarize growth when *RGA2^{8A}* is overexpressed. Indeed, Cdc42p fails to localize to a discrete site in unbudded cells when *RGA2^{8A}* is overexpressed (Supplementary Figure 5). Confocal microscopy also revealed an overlapping localization for Rga2^{8A}p and Cdc42p in small-budded *cln1*Δ*cln2*Δ cells (Figure 7B). A hyperactive Rga2^{8A}p–Cdc42p complex could interfere with cycling of Cdc42p-GTP/GDP, which is required for promoting all the aspects of polarizing growth (Caviston *et al*, 2002; Gladfelter *et al*, 2002; Irazoqui *et al*, 2003; Court and Sudbery, 2007) This idea is supported by failure of overexpressed *CDC24* or *CDC42^{G12V}* (constitutively active Cdc42p) to rescue the toxicity associated with *RGA2^{8A}* overexpression (data not shown). Rga2p phosphorylation may influence its GAP activity and/or physical interaction with Cdc42p. While we have been able to co-immunoprecipitate Rga2^{8A}p with the Pcls (data not shown), we have been unable to detect a stabilized interaction between Rga2^{8A}p and Cdc42p (data not shown).

Our data suggest a role for G1-phase CDKs in downregulating Cdc42 GAP activity to ensure appropriate Cdc42p activation during G1 phase. Inhibition of GAPs by CDKs may be a general mechanism to regulate the actin cytoskeleton. For example, the highly elongated morphology of hyphae in *Candida albicans* is due to increased activity of Cdc42p and deletion of the GAPs *RGA2*, and *BEM3* results in the elongation of pseudohyphal cells (Court and Sudbery, 2007). Rga2p is phosphorylated in a hyphal-specific manner in *C. albicans*, indicating that phosphorylation likely inhibits Rga2p during this stage of the *Candida* life cycle (Court and Sudbery, 2007). The phosphorylation of mammalian GAPs also alters cytoskeletal network organization and signal transduction; a Cdc42 and Rac1 GAP, CdGAP, is phosphorylated by ERK1/2 *in vivo*, leading to downregulation of CdGAP activity and consequent Rac1 activation, and cytoskeletal remodeling (Tcherkezian *et al*, 2005). Likewise, activity of the Cdc42 and Rac1 GAP, RICS, is inhibited via phosphorylation by calcium/calmodulin-dependent kinase II (Okabe *et al*, 2003). In general, regulation of Cdc42p and other Rho-type GTPase modules by CDKs may serve to connect cues from the

©2007 European Molecular Biology Organization

cell cycle and the actin cytoskeleton to coordinate cell surface growth with cell division. Given the conservation of Rho-type GTPase pathways, regulatory events uncovered in yeast are likely relevant in other eukaryotes.

Materials and methods

Yeast strains and plasmids (Tables II and III)

Standard yeast growth conditions were used. All yeast gene disruptions were achieved by homologous recombination by standard polymerase chain reaction (PCR)-based methods, and verified by PCR and phenotypic analyses. Point mutants were made using PCR-based site-directed mutagenesis and confirmed by sequencing. Cell size analysis and synchronization were performed as described (Costanzo *et al*, 2004).

Microscopy

Cells were photographed with a CoolSNAP HQ high-speed digital camera (Roeper Scientific) mounted on a Leica DM-LB microscope. Images were captured and analyzed using MetaMorph software (Universal Imaging Media, PA). For confocal microscopy, proteins were visualized with a Leica DMI 6000B fluorescence microscope equipped with a spinning-disc head and an argon laser (458, 488, and 514 nm) (Quorum Technologies), and an ImagEM-CCD camera (Hamamatsu, Japan), and analyzed using Volocity software (distributed by Quorum Technologies Inc., Guelph, ON). Z-stacks of 10 spinning-disc confocal images separated by 0.2 μm were taken.

Kinase assays and mass spectrometry

Recombinant Pcl–Pho85p and Cln2p–Cdc28p kinases were expressed and purified from insect cells as described (Huang *et al*, 1999). Substrates included 150 ng of five truncated versions of Rga2p: amino acids 1–240, 233–365, 357–658, 652–795, and 789–1009 (all N-terminal GST fusions were expressed in *Escherichia coli* and purified using glutathione–Sepharose columns). Kinase reactions were performed as described (Costanzo *et al*, 2004). Details of the methods for purifying and processing phosphorylated proteins for mass spectrometry are available at the Andrews lab website (www.utoronto.ca/andrewslab/).

Cdc42 activation assay

GTP-bound Cdc42p in different lysates overexpressing *CDC24* was detected using a GST-PAK (a GST fusion of the CRIB domain from

Table III Plasmids used in this study

Plasmid	Description	Reference or source
pEGH	p*GAL1/10*-GST-6xHis *URA3* 2μ	Zhu *et al* (2000)
pGST-*RGA2*	pEGH + *RGA2*	Zhu *et al* (2000)
p*GAL1*-*CFLAG*	p*GAL1-FLAG LEU2* CEN	Ho *et al* (2002)
pBA2059	p*GAL1 RGA2-FLAG*	This study
pBA2060	p*GAL RGA2^{8A}-FLAG*	This study
pBA2195	p*GAL RGA2^{8A,K872A}-FLAG*	This study
pE127	pRS316-*GAL1-CDC24*	Tcherkezian *et al* (2005)
pRS426	*URA3* 2μ	R Sikorski
pJM35	pRS426-*PCL2*pr-GFP-*PCL2*	Moffat and Andrews (2004)
pJM40	pRS426-*PCL1*pr-GFP-*PCL1*	Moffat and Andrews (2004)
pJM36	pRS426-*PCL9*pr-GFP-*PCL9*	Andrews lab
pBA2046	pDEST15 GST-*RGA2* (aa 1–240)	This study
pBA2047	pDEST15 GST-*RGA2* (aa 233–365)	This study
pBA2048	pDEST15 GST-*RGA2* (aa 357–658)	This study
pBA2049	pDEST15 GST-*RGA2* (aa 652–795)	This study
pBA2050	pDEST15 GST-*RGA2* (aa 789–1009)	This study
pBA2123	p*GAL*-13xMYC-*PCL1 URA3* 2μ	Andrews lab
pBA2124	p*GAL*-13xMYC-*PCL2 URA3* 2μ	Andrews lab
pBA2125	p*GAL*-13xMYC-*PCL9 URA3* 2μ	Andrews lab
pBA2220	p*MET25-mcherry*-GAAAAAAAG-*CDC42 URA3* CEN	This study

Table II *Saccharomyces cerevisiae* strains used in this study

Strain(s)	Genotype	Reference or source
BY263	*MAT***a** *trp1 leu2 his3 ura3 lys2 ade2*	Measday *et al* (1997)
BY391	*MAT***a** *pho85ΔLEU2 trp1 leu2 his3 ura3 lys2 ade2*	Measday *et al* (1997)
BY435	*MAT***a** *pcl1ΔHIS3 trp1 leu2 his3 ura3 lys2 ade2*	Andrews lab
BY451	*MAT***a** *pcl2ΔLYS2 trp1 leu2 his3 ura3 lys2 ade2*	Andrews lab
BY694	*MAT***a** *pcl9ΔHIS3 trp1 leu2 his3 ura3 lys2 ade2*	Measday *et al* (1997)
BY425	*MAT***a** *pcl1ΔHIS3 pcl2ΔLYS2 trp1 leu2 his3 ura3 lys2 ade2*	Andrews lab
BY697	*MAT***a** *pcl2ΔLYS2 pcl9ΔHIS3 trp1 leu2 his3 ura3 lys2 ade2*	Andrews lab
BY4020	*MAT***a** *pcl1ΔHIS3 pcl9ΔHPH trp1 leu2 his3 ura3 lys2 ade2*	This study
BY4334	*MAT***a** *pcl1ΔHIS3 pcl2ΔLYS2 pcl9ΔHPH trp1 leu2 his3 ura3 lys2 ade2*	This study
BY438	*MAT***a** *cln1ΔTRP1 cln2ΔURA3 trp1 leu2 his3 ura3 lys2 ade2*	Andrews lab
Y4741	*MAT***a** *ura3Δ0 leu2Δ0 his3Δ1 met15Δ0*	Winzeler *et al* (1999)
Y7031	*MAT***a** *can1ΔSTE2pr-HIS3 lyp1Δ cyh2 ura3Δ0 leu2Δ0 his3Δ1 met15Δ0 LYS2$^+$*	C Boone
BY4345	Y7031 *MATα pho85ΔNAT*	This study
BY4033	*MATα cln1ΔNAT cln2Δ HPH ura3Δ0 leu2Δ0 can1ΔMFA1pr-HIS3 his3Δ1 lys2Δ0 MET15$^+$*	This study
BY4004	*MAT***a** *RGA2*-TAP::*HIS3 ura3Δ0 leu2Δ0 his3Δ1 lys2Δ0 MET15$^+$*	Ghaemmaghami *et al* (2003)
BY4325	*MAT***a** *RGA2*-GFP::*HIS3 ura3Δ0 leu2Δ0 his3Δ1 lys2Δ0 MET15$^+$*	Huh *et al* (2003)
BY4188	*MAT***a** *RGA2^{8A}*-TAP::*HIS3 ura3Δ0 leu2Δ0 his3Δ1 lys2Δ0 MET15$^+$*	This study
BY4288	*MAT***a** *RGA2^{8A}*-GFP::*HIS3 ura3Δ0 leu2Δ0 his3Δ1 lys2Δ0 MET15$^+$*	This study
BY4053	*MAT***a** *bem3ΔKAN rga2ΔNAT rga1ΔHPH ura3Δ0 leu2Δ0 his3Δ1 lys2Δ0 MET15$^+$*	This study
BY4287	*MAT***a** *bem3ΔKAN RGA2^{8A}*-GFP::*HIS3 rga1ΔHPH ura3Δ0 leu2Δ0 his3Δ1 lys2Δ0 MET15$^+$*	This study
YEF313	*MAT***a** *cdc24-4 ade2 trp1 leu2 ura3 his3 lys2*	E Bi
BY4141	*MAT***a** *pho85as*::*HPH RGA2*-TAP::*HIS3 ura3Δ0 leu2Δ0 his3Δ1 lys2Δ0 met15Δ0*	This study
BY4140	*MAT***a** *cdc28as1*::*HPH RGA2*-TAP::*HIS3 ura3Δ0 leu2Δ0 his3Δ1 lys2Δ0 met15Δ0*	This study
BY4103	*MAT***a** *RGA2*-TAP::*HIS3 cln1ΔNAT cln2Δ HPH ura3Δ0 leu2Δ0 his3Δ1 lys2Δ0 MET15$^+$*	This study
BY4281	*MAT***a** *RGA2^{8A}*-TAP::*HIS3 cln1ΔNAT cln2Δ HPH ura3Δ0 leu2Δ0 his3Δ1 lys2Δ0 MET15$^+$*	This study
BY4099	*MAT***a** *RGA2*-GFP::*HIS3 cln1ΔNAT cln2Δ HPH ura3Δ0 leu2Δ0 his3Δ1 lys2Δ0 MET15$^+$*	This study
BY4283	*MAT***a** *RGA2^{8A}*-GFP::*HIS3 cln1ΔNAT cln2Δ HPH ura3Δ0 leu2Δ0 his3Δ1 lys2Δ0 MET15$^+$*	This study
BY4091	*MAT***a** *pcl1ΔNAT pcl2ΔHPH pcl9ΔKAN ura3Δ0 leu2Δ0 his3Δ1 lys2Δ0 met15Δ0*	This study
BY2456	*MAT***a** *cdc24-4 pcl1ΔLEU KAN-GALp-3xHA-PCL2 ade2 trp1 leu2 ura3 his3 lys2*	J Moffat
BY4388	*MATα cdc24-4 RGA2^{8A}*-GFP::*HIS3*	This study

©2007 European Molecular Biology Organization

human Pak1) pull-down assay adapted from Caviston *et al* (2002) and Aguilar *et al* (2006).

Antibodies, immunoprecipitation, and immunoblotting

Western blotting was performed using monoclonal α-myc 9E10 (produced by University of Toronto monoclonal antibody facility), polyclonal α-TAP (Open Biosystems), polyclonal anti-Cdc42 antibody (Santa Cruz Biotechnology, sc-87), and monoclonal α-Flag M2 (Sigma) antibodies. For immunoprecipitation, cells were disrupted in lysis buffer (50 mM Tris–HCl, pH 7.5, 100 mM NaCl, 1 mM EDTA, 5 mM NaF, and protease inhibitors) and clarified by centrifugation at 13k r.p.m. for 10 min. Extracts were diluted with IP buffer (50 mM Tris–HCl, pH 7.5, 100 mM NaCl, 1% Triton X-100, 5 mM NaF, and protease inhibitors) and incubated with IgG sepharose (Amersham Biosciences). Resin was washed 3 × with IP buffer and resuspended in 2 × sample buffer. Extract and supernatant from resin were separated by electrophoresis on an SDS/8% polyacrylamide gel and transferred to PVDF membrane for Western blotting. Samples to be treated with lambda phosphatase were washed 2 × and resuspended in 200 μl buffer (2 mM $MnCl_2$, 100 mM NaCl, 2 mM DTT, 0.1 mM EGTA, 0.01% Brij 35, and 50 mM Tris–HCl, pH 8.0).

Supplementary data

Supplementary data are available at *The EMBO Journal* Online (http://www.embojournal.org).

Acknowledgements

RS was supported by a Terry Fox Foundation research studentship from the National Cancer Institute of Canada. This work was supported by grants from the Canadian Institutes of Health Research, the National Cancer Institute of Canada, and Genome Canada through the Ontario Genomics Institute to BA. DF and JS acknowledge financial support from the Canadian Foundation for Innovation, the Province of Ontario, the Canada Research Chair Program, NSERC, CIHR, the University of Ottawa, MDS Inc., and the Foundation Louis-Lévesque.

References

Aguilar RC, Longhi SA, Shaw JD, Yeh LY, Kim S, Schon A, Freire E, Hsu A, McCormick WK, Watson HA, Wendland B (2006) Epsin N-terminal homology domains perform an essential function regulating Cdc42 through binding Cdc42 GTPase-activating proteins. *Proc Natl Acad Sci USA* **103:** 4116–4121

Archambault V, Chang EJ, Drapkin BJ, Cross FR, Chait BT, Rout MP (2004) Targeted proteomic study of the cyclin–Cdk module. *Mol Cell* **14:** 699–711

Benton BK, Tinkelenberg AH, Jean D, Plump SD, Cross FR (1993) Genetic analysis of Cln/Cdc28 regulation of cell morphogenesis in budding yeast. *EMBO J* **12:** 5267–5275

Bishop AC, Ubersax JA, Petsch DT, Matheos DP, Gray NS, Blethrow J, Shimizu E, Tsien JZ, Schultz PG, Rose MD, Wood JL, Morgan DO, Shokat KM (2000) A chemical switch for inhibitor-sensitive alleles of any protein kinase. *Nature* **407:** 395–401

Bloom J, Cross FR (2007) Multiple levels of cyclin specificity in cell-cycle control. *Nat Rev Mol Cell Biol* **8:** 149–160

Butty AC, Perrinjaquet N, Petit A, Jaquenoud M, Segall JE, Hofmann K, Zwahlen C, Peter M (2002) A positive feedback loop stabilizes the guanine-nucleotide exchange factor Cdc24 at sites of polarization. *EMBO J* **21:** 1565–1576

Carroll AS, Bishop AC, DeRisi JL, Shokat KM, O'Shea EK (2001) Chemical inhibition of the Pho85 cyclin-dependent kinase reveals a role in the environmental stress response. *Proc Natl Acad Sci USA* **98:** 12578–12583

Caviston JP, Longtine M, Pringle JR, Bi E (2003) The role of Cdc42p GTPase-activating proteins in assembly of the septin ring in yeast. *Mol Biol Cell* **14:** 4051–4066

Caviston JP, Tcheperegine SE, Bi E (2002) Singularity in budding: a role for the evolutionarily conserved small GTPase Cdc42p. *Proc Natl Acad Sci USA* **99:** 12185–12190

Clark EA, Golub TR, Lander ES, Hynes RO (2000) Genomic analysis of metastasis reveals an essential role for RhoC. *Nature* **406:** 532–535

Costanzo M, Nishikawa JL, Tang X, Millman JS, Schub O, Breitkreuz K, Dewar D, Rupes I, Andrews B, Tyers M (2004) CDK activity antagonizes Whi5, an inhibitor of G1/S transcription in yeast. *Cell* **117:** 899–913

Court H, Sudbery P (2007) Regulation of Cdc42 GTPase activity in the formation of Hyphae in *Candida albicans*. *Mol Biol Cell* **18:** 265–281

Cvrckova F, Nasmyth K (1993) Yeast G1 cyclins CLN1 and CLN2 and a GAP-like protein have a role in bud formation. *EMBO J* **12:** 5277–5286

de Bruin RA, McDonald WH, Kalashnikova TI, Yates III J, Wittenberg C (2004) Cln3 activates G1-specific transcription via phosphorylation of the SBF bound repressor Whi5. *Cell* **117:** 887–898

Etienne-Manneville S (2004) Cdc42—the centre of polarity. *J Cell Sci* **117:** 1291–1300

Frame MC, Brunton VG (2002) Advances in Rho-dependent actin regulation and oncogenic transformation. *Curr Opin Genet Dev* **12:** 36–43

Friesen H, Murphy K, Breitkreutz A, Tyers M, Andrews B (2003) Regulation of the yeast amphiphysin homologue Rvs167p by phosphorylation. *Mol Biol Cell* **14:** 3027–3040

Ghaemmaghami S, Huh WK, Bower K, Howson RW, Belle A, Dephoure N, O'Shea EK, Weissman JS (2003) Global analysis of protein expression in yeast. *Nature* **425:** 737–741

Gladfelter AS, Bose I, Zyla TR, Bardes ES, Lew DJ (2002) Septin ring assembly involves cycles of GTP loading and hydrolysis by Cdc42p. *J Cell Biol* **156:** 315–326

Gulli MP, Jaquenoud M, Shimada Y, Niederhauser G, Wiget P, Peter M (2000) Phosphorylation of the Cdc42 exchange factor Cdc24 by the PAK-like kinase Cla4 may regulate polarized growth in yeast. *Mol Cell* **6:** 1155–1167

Hartwell LH, Culotti J, Pringle JR, Reid BJ (1974) Genetic control of the cell division cycle in yeast. *Science* **183:** 46–51

Henchoz S, Chi Y, Catarin B, Herskowitz I, Deshaies RJ, Peter M (1997) Phosphorylation- and ubiquitin-dependent degradation of the cyclin-dependent kinase inhibitor Far1p in budding yeast. *Genes Dev* **11:** 3046–3060

Ho Y, Gruhler A, Heilbut A, Bader GD, Moore L, Adams SL, Millar A, Taylor P, Bennett K, Boutilier K, Yang L, Wolting C, Donaldson I, Schandorff S, Shewnarane J, Vo M, Taggart J, Goudreault M, Muskat B, Alfarano C *et al* (2002) Systematic identification of protein complexes in *Saccharomyces cerevisiae* by mass spectrometry. *Nature* **415:** 180–183

Huang D, Moffat J, Andrews B (2002) Dissection of a complex phenotype by functional genomics reveals roles for the yeast cyclin-dependent protein kinase Pho85 in stress adaptation and cell integrity. *Mol Cell Biol* **22:** 5076–5088

Huang D, Moffat J, Wilson WA, Moore L, Cheng C, Roach PJ, Andrews B (1998) Cyclin partners determine Pho85 protein kinase substrate specificity *in vitro* and *in vivo*: control of glycogen biosynthesis by Pcl8 and Pcl10. *Mol Cell Biol* **18:** 3289–3299

Huang D, Patrick G, Moffat J, Tsai LH, Andrews B (1999) Mammalian Cdk5 is a functional homologue of the budding yeast Pho85 cyclin-dependent protein kinase. *Proc Natl Acad Sci USA* **96:** 14445–14450

Huh WK, Falvo JV, Gerke LC, Carroll AS, Howson RW, Weissman JS, O'Shea EK (2003) Global analysis of protein localization in budding yeast. *Nature* **425:** 686–691

Irazoqui JE, Gladfelter AS, Lew DJ (2003) Scaffold-mediated symmetry breaking by Cdc42p. *Nat Cell Biol* **5:** 1062–1070

Johnson DI (1999) Cdc42: an essential Rho-type GTPase controlling eukaryotic cell polarity. *Microbiol Mol Biol Rev* **63:** 54–105

Kozminski KG, Chen AJ, Rodal AA, Drubin DG (2000) Functions and functional domains of the GTPase Cdc42p. *Mol Biol Cell* **11:** 339–354

Lenburg ME, O'Shea EK (2001) Genetic evidence for a morphogenetic function of the *Saccharomyces cerevisiae* Pho85 cyclin-dependent kinase. *Genetics* **157:** 39–51

Li R, Zhang B, Zheng Y (1997) Structural determinants required for the interaction between Rho GTPase and the GTPase-activating domain of p190. *J Biol Chem* **272:** 32830–32835

©2007 European Molecular Biology Organization

Marquitz AR, Harrison JC, Bose I, Zyla TR, McMillan JN, Lew DJ (2002) The Rho-GAP Bem2p plays a GAP-independent role in the morphogenesis checkpoint. *EMBO J* **21:** 4012–4025

McCusker D, Denison C, Anderson S, Egelhofer TA, Yates III JR, Gygi SP, Kellogg DR (2007) Cdk1 coordinates cell-surface growth with the cell cycle. *Nat Cell Biol* **9:** 506–515

Measday V, Moore L, Retnakaran R, Lee J, Donoviel M, Neiman AM, Andrews B (1997) A family of cyclin-like proteins that interact with the Pho85 cyclin-dependent kinase. *Mol Cell Biol* **17:** 1212–1223

Miller ME, Cross FR (2001) Cyclin specificity: how many wheels do you need on a unicycle? *J Cell Sci* **114:** 1811–1820

Moffat J, Andrews B (2004) Late-G1 cyclin-CDK activity is essential for control of cell morphogenesis in budding yeast. *Nat Cell Biol* **6:** 59–66

Moffat J, Huang D, Andrews B (2000) Functions of Pho85 cyclin-dependent kinases in budding yeast. *Prog Cell Cycle Res* **4:** 97–106

Moses AM, Heriche JK, Durbin R (2007) Clustering of phosphorylation site recognition motifs can be exploited to predict the targets of cyclin-dependent kinase. *Genome Biol* **8:** R23

Nern A, Arkowitz RA (2000) Nucleocytoplasmic shuttling of the Cdc42p exchange factor Cdc24p. *J Cell Biol* **148:** 1115–1122

Nishizawa M, Kawasumi M, Fujino M, Toh-e A (1998) Phosphorylation of sic1, a cyclin-dependent kinase (Cdk) inhibitor, by Cdk including Pho85 kinase is required for its prompt degradation. *Mol Biol Cell* **9:** 2393–2405

Okabe T, Nakamura T, Nishimura YN, Kohu K, Ohwada S, Morishita Y, Akiyama T (2003) RICS, a novel GTPase-activating protein for Cdc42 and Rac1, is involved in the beta-catenin-N-cadherin and *N*-methyl-D-aspartate receptor signaling. *J Biol Chem* **278:** 9920–9927

Pawlak G, Helfman DM (2001) Cytoskeletal changes in cell transformation and tumorigenesis. *Curr Opin Genet Dev* **11:** 41–47

Pruyne D, Bretscher A (2000a) Polarization of cell growth in yeast. *J Cell Sci* **113** (Pt 4)**:** 571–585

Pruyne D, Bretscher A (2000b) Polarization of cell growth in yeast. I. Establishment and maintenance of polarity states. *J Cell Sci* **113** (Pt 3)**:** 365–375

Ptacek J, Devgan G, Michaud G, Zhu H, Zhu X, Fasolo J, Guo H, Jona G, Breitkreutz A, Sopko R, McCartney RR, Schmidt MC, Rachidi N, Lee SJ, Mah AS, Meng L, Stark MJ, Stern DF, De Virgilio C, Tyers M *et al* (2005) Global analysis of protein phosphorylation in yeast. *Nature* **438:** 679–684

Richman TJ, Sawyer MM, Johnson DI (2002) *Saccharomyces cerevisiae* Cdc42p localizes to cellular membranes and clusters at sites of polarized growth. *Eukaryot Cell* **1:** 458–468

Schwob E, Bohm T, Mendenhall MD, Nasmyth K (1994) The B-type cyclin kinase inhibitor p40SIC1 controls the G1 to S transition in *S. cerevisiae*. *Cell* **79:** 233–244

Shimada Y, Gulli MP, Peter M (2000) Nuclear sequestration of the exchange factor Cdc24 by Far1 regulates cell polarity during yeast mating. *Nat Cell Biol* **2:** 117–124

Shimada Y, Wiget P, Gulli MP, Bi E, Peter M (2004) The nucleotide exchange factor Cdc24p may be regulated by auto-inhibition. *EMBO J* **23:** 1051–1062

Sloat BF, Adams A, Pringle JR (1981) Roles of the CDC24 gene product in cellular morphogenesis during the *Saccharomyces cerevisiae* cell cycle. *J Cell Biol* **89:** 395–405

Smith GR, Givan SA, Cullen P, Sprague Jr GF (2002) GTPase-activating proteins for Cdc42. *Eukaryot Cell* **1:** 469–480

Sopko R, Huang D, Preston N, Chua G, Papp B, Kafadar K, Snyder M, Oliver SG, Cyert M, Hughes TR, Boone C, Andrews B (2006) Mapping pathways and phenotypes by systematic gene overexpression. *Mol Cell* **21:** 319–330

Tcherkezian J, Danek EI, Jenna S, Triki I, Lamarche-Vane N (2005) Extracellular signal-regulated kinase 1 interacts with and phosphorylates CdGAP at an important regulatory site. *Mol Cell Biol* **25:** 6314–6329

Toenjes KA, Sawyer MM, Johnson DI (1999) The guanine-nucleotide-exchange factor Cdc24p is targeted to the nucleus and polarized growth sites. *Curr Biol* **9:** 1183–1186

Ubersax JA, Woodbury EL, Quang PN, Paraz M, Blethrow JD, Shah K, Shokat KM, Morgan DO (2003) Targets of the cyclin-dependent kinase Cdk1. *Nature* **425:** 859–864

Winzeler EA, Shoemaker DD, Astromoff A, Liang H, Anderson K, Andre B, Bangham R, Benito R, Boeke JD, Bussey H, Chu AM, Connelly C, Davis K, Dietrich F, Dow SW, El Bakkoury M, Foury F, Friend SH, Gentalen E, Giaever G *et al* (1999) Functional characterization of the *S. cerevisiae* genome by gene deletion and parallel analysis. Science **285:** 901–906

Yoshida S, Kono K, Lowery DM, Bartolini S, Yaffe MB, Ohya Y, Pellman D (2006) Polo-like kinase Cdc5 controls the local activation of Rho1 to promote cytokinesis. *Science* **313:** 108–111

Zheng Y, Cerione R, Bender A (1994) Control of the yeast bud-site assembly GTPase Cdc42. Catalysis of guanine nucleotide exchange by Cdc24 and stimulation of GTPase activity by Bem3. *J Biol Chem* **269:** 2369–2372

Zhu H, Klemic JF, Chang S, Bertone P, Casamayor A, Klemic KG, Smith D, Gerstein M, Reed MA, Snyder M (2000) Analysis of yeast protein kinases using protein chips. *Nat Genet* **26:** 283–289

 ©2007 European Molecular Biology Organization